Interactions between Evaporating Droplets in a Monodisperse Stream

B. Frackowiak[1*], G. Lavergne[2], C. Tropea[1], A. Strzelecki[2]
[1]Technische Universität Darmstadt, SLA
Petersenstraße 30, D-64287, Darmstadt, Germany
[2]ONERA, DMAE
2 avenue Edouard Belin, 31055, Toulouse, France

Abstract

A numerical simulation of the evaporation in a monodisperse droplet stream is conducted, taking into account the interactions between droplets. A code solving the Navier-Stokes equations in the liquid phase is coupled to the calculations of the external flow using different CFD softwares. The transient stage of the evaporation, and the non-uniform transfer parameters on the droplet surface are taken into account. The results are validated with the experimental measurements of the vapor mole fraction field and with empirical correlations on the transfer parameters. This investigation emphasizes the strong interaction effects between closely spaced droplets in a dense spray, reducing significantly the transfer parameters. The Marangoni force in the droplet becomes more significant than the viscous force, driving the internal motion of the droplet and affecting the temperature field. Finally, a better understanding of the evaporation phenomenon with closely spaced droplets will help to refine existing models used in dense sprays.

Introduction

Droplet evaporation modeling in dense sprays is indispensable for providing accurate simulations in combustion chambers. However, the evaporation phenomenon is complex and hypotheses must be made to ensure reasonable computation time. The spray is divided into droplet parcels, each parcel being affected by the same drag coefficient, vapor mass flow rate and total heat flux, as with a single droplet. These transfer parameters are calculated according to empirical correlations [1,2], whereas simplified evaporation models assuming spherical symmetry yield the droplet temperature and diameter.

However, the interactions between closely spaced droplets in dense sprays affect their evaporation, reducing significantly the transfer parameters compared with the case of an isolated droplet. Furthermore, the transient stage of droplet evaporation must be considered in the liquid phase modeling, in particular over the short penetration distances of a spray in a combustion chamber [3]. Therefore, a Direct Numerical Simulation (DNS) carried out by Chiang and Sirignano [4] around three aligned droplets suggested a corrective factor η_1 concerning the 3rd droplet applied to the Chiang drag coefficient used in the isolated droplet case [5]. Moreover, measurements have been carried out by Atthasit and Virepinte [6,7] around a monodisperse droplet stream, generated with a piezoelectric ceramic exciter, which leads to Rayleigh break-up of the liquid jet (Fig. 1). Each droplet has the same diameter D_d, the same velocity $V_{droplet}$, the same temperature and the same spacing parameter $C=S_d/D_d$ at a given distance from the injector, S_d being the distance between two consecutive droplets. The spacing parameter C can be modified by changing the excitation frequency. These measurements at different downstream positions have provided the temporal evolution of effectively a single droplet in the jet, and resulted in corrective factors η_1 for the drag coefficient [1,6] and η_2 for the mass flow rate and total heat flux [2,6,7]. Computations by Leiroz [8] around an infinite jet in stagnant air have resulted in an alternative corrective factor η_2, considering only diffusion.

$$\eta_{1\text{Chiang}} = 0.434 \times C^{1.85} \qquad (1)$$

$$\eta_{1\text{Virepinte}} = 1 - 0.86 \times \exp(-0.053 \times C) \qquad (2)$$

$$\eta_{2\text{Virepinte}} = 1 - 0.42 \times \left[1 - \frac{\exp(-0.19 \times (C-5)) - \exp(-0.6 \times (C-5))}{\exp(-0.19 \times (C-5)) + \exp(-0.6 \times (C-5))} \right] \qquad (3)$$

*Corresponding author

$$\eta_{2\text{Atthasit}} = 1 - 0.57 \times \left[1 - \frac{1 - \exp\left(-0.13 \times (C-6)\right)}{1 + \exp\left(-0.13 \times (C-6)\right)} \right] \quad (4)$$

$$\eta_{2\text{Leiroz}} = 1 - 0.6328 \times C^{-0.8782} \quad (5)$$

Most measurements in such experiments are performed using non-intrusive optical techniques, which are very sensitive to the internal temperature fields inside the droplets. Numerical investigations have also been carried out to predict these internal fields, affected by the convection induced by the droplet motion. In the Hill Vortex model [9], the complete energy equation is computed with a given velocity profile modelling the vortex shaped liquid motion. The transfer parameters are uniform at the droplet surface, provided by the common correlations [1,2], whereas the liquid maximal velocity is proportional to the friction coefficient. The strong influence of the internal motion on the heat transfer inside the droplet is highlighted in the temperature fields, starting from spherically symmetric fields to fields following the motion streamlines. Castanet et al. [10,11] have extended this model to the monodisperse stream, using a computational domain around one droplet in an Eulerian approach for the gas phase, with a periodic boundary condition at the inlet and outlet. A good agreement with the experimental measurements has been obtained regarding the temperature field inside the droplet and the vapor mole fraction field.

Otherwise, non-uniform transfer parameter have been investigated by Dwyer et al. [12,13] on an isolated droplet or on droplet clusters, taking into account the Marangoni effect. This phenomenon results from the dependence of the surface tension on temperature which creates a stress additional to the viscous stress, affecting the liquid motion and consequently the temperature fields inside the droplet.

The proposed simulation aims to investigate more precisely the transient stage of the evaporation phenomenon in a monodisperse stream, in order to capture the external vapor mole fraction field as well as the temperature field in the droplet, taking into account the Marangoni effect with non-uniform transfer parameters on the surface.

Proposed numerical simulation

The proposed simulation is based on two-way coupling between the external flow computations with the CFD softwares *Fluent* or *OpenFOAM* [14], and a code solving the time dependent Navier-Stokes equations for the droplet internal fields. The configuration is axisymmetric. The interface remains spherical due to low Weber numbers, and the radiative heat transfer, the gravity, the pressure force work, the gas solubility in the liquid phase and the heat resulting from viscous dissipation are neglected.

The gas phase is computed considering each droplet as a rigid mass flow source supplying a second species to the surrounding laminar air flow. A reduced domain between two consecutives droplets is considered, using an Eulerian approach (Fig.1), similar to the simulation proposed by Castanet et al. [11]. Periodic boundary conditions are set between the inlet and the outlet, relying on a characteristic distance of the aerodynamic field several orders of magnitude larger than the distance between two consecutive droplets. Otherwise, the right far-field boundary condition corresponds to a uniform dry air flow evolving at the real droplet velocity in the experimental jet. The spacing parameter *C* and the droplet diameter are constant. Only one droplet is considered for the liquid phase, whose leading edge and trailing edge correspond respectively to the downstream and upstream half droplet surfaces.

At the droplet surface, the radial species, temperature and momentum radial gradients yield the mass flow rate $\dot{m}$, effective heat flux $Ql_{\text{effective}}$ and viscous stress profiles, by applying the local conservation equations, including the Soret effect modelled with the coefficient D_{Tvap} and neglecting the tangential gradients according to the boundary layer hypothesis. The temperature profile is deduced from the computations in the liquid phase, and the vapor mass fraction profile is equal to its saturation value. The dependence of the surface tension σ on the temperature results in the Marangoni stress profile [12,13] which is added to the viscous one, providing the total stress τ_p.

$$\dot{m} = -\frac{1}{1 - Y_{vap}} \times \left[\rho_{vap} D_{vap} \frac{\partial Y_{vap}}{\partial r} + \frac{D_{Tvap}}{T} \times \frac{\partial T}{\partial r} \right] \quad (6)$$

$$Ql_{effective} = \lambda_{vap} \frac{\partial T}{\partial r} - L_V . \dot{m} \quad (7)$$

$$\tau_p = \mu_{vap} \frac{\partial v_\theta}{\partial r} + \frac{2}{D_d} \times \frac{\partial \sigma}{\partial T} \times \frac{\partial T}{\partial \theta} \quad (8)$$

The liquid phase is treated as a single component. The Navier-Stokes equation are solved assuming incompressible flow and using the projection method [15] to insure a velocity field with null divergence and satisfying the continuity equation. The numerical resolution implies finite volumes and finite differences schemes respectively for the momentum and the temperature, with a semi – implicit Crank Nicholson time resolution for the diffusive terms.

$$\iiint_{\Omega} \frac{\partial}{\partial t}\left(\rho_{liq}\vec{v}\right) d\omega + \iint_{\Sigma} \rho_{liq}\vec{v}\left(\vec{v}.\vec{n}\right) dS + \iint_{\Sigma} \left(\vec{\vec{pI}} - \mu_{liq}.\vec{grad}\left(\vec{v}\right)\right).d\vec{S} = \vec{0} \qquad (9)$$

$$\rho_{liq}C_{pliq}\frac{\partial T}{\partial t} + \rho_{liq}C_{pliq}.\left(\vec{v}.\vec{grad}\left(T\right)\right) - \lambda_{liq}\Delta T = 0 \qquad (10)$$

The quasi-static evaporation hypothesis is adopted for the two-way coupling: the momentum, the mass and the heat transfer at the droplet surface are immediately adapted to the local boundary conditions. This hypothesis leads to an update of the boundary conditions during the evaporation at a longer period than the time step in both phases.

Nevertheless, the simulation of a monodisperse stream is challenging, because a steady state is only reached when the entrained air counteracts the vapor diffusion from the droplet surface. And this significant phenomenon cannot be taken into account under an Eulerian approach [11] with fixed droplets. Therefore, the entrained air is estimated in a larger scale by using a Lagrangian approach, where the droplet stream is considered as a cylinder moving at the average droplet velocity (Fig.1). The cylinder is a mass flow source whose flow rate, temperature and vapor mole fraction are the same as at the droplet surface. The upstream far-field boundaries of the domain corresponds to pressure inlets, knowing the ambient temperature and pressure of the room. A distance range from the injector is defined between L_{min} and L_{max} on the liquid cylinder, corresponding to the experimental investigated zone. The time range between $t_{min} = L_{min}/V_{droplet}$ and $t_{max} = L_{max}/V_{droplet}$ is also considered for the computation between the two consecutives droplets.

In the periodic domain, the time varying external flow, initially uniform and dry, evolves continuously due to the temperature, momentum and species transport, whereas the droplet temperature and velocity fields are reset to their uniform values at every period T_f . The process can be interpreted as successive simulations n, each one during a time T_f , with new initial conditions for the liquid phase, but without modifying the final field of the simulation $n - 1$ for the gas phase. When the best fit between the vapor mole fraction fields around the cylinder and in the periodic domain is obtained, respectively between L_{min} and L_{max} and between t_{min} and t_{max}, the process is stopped. The last simulation yields external fields in agreement with the entrained air and capturing precisely the interactions between close droplets. The period T_f is fixed to 5 ms for all the simulations.

Results and Discussion

The conditions for which the droplet stream has been simulated correspond to those for which experimental data is available. In particular, a Planar Laser Induced Fluorescence (PLIF) technique has been developed around acetone monodisperse droplet streams [16], especially for the cooling cases mentioned in Table 1. Attention is focused first on the vapor mole fraction profiles, corresponding to the droplet equatorial plane, perpendicular to the stream direction.

A first comparison between the vapor mole fraction profiles extracted around the cylinder and in the periodic domain (Fig. 2,a) highlights the relevancy of this criteria used to control the vapor accumulation in the periodic domain, in agreement with the entrained air. For comparison with the experimental measurements (Fig. 2, b), the computed profiles are averaged over the sheet thickness, in order to take into account the depth of field of the camera. The quantitative experimental measurements concur with the numerical results, except in the area close to the droplet surface: experimental results are not available in this region due to the presence of a mask to eliminate the blooming effect from the liquid phase [16].

A comparison of the average transfer parameters values with the empirical correlations is shown in Fig. 3. The comparison with the Renkzizbulut [1] and Ranz-Marshall [2] correlation emphasizes the strong decrease of the transfer parameters due to interaction effects. The overestimation with the Chiang correction (Eq. 1) [4] highlights the fact that interactions between droplets were not accounted for. The best agreement is obtained with the Virepinte (Eq. 2, 3) [6] and Atthasit (Eq. 4) [7] corrections. Moreover, the vapor flow rate provided by the proposed simulation would have yielded respective diameter decreases of 1% and 2% for the droplets injected at 22.4°C and 45.6°C, after 5 ms. This retroactively justifies the constant diameter hypothesis.

The Marangoni stress becomes significant when the surface temperature gradient increases, compared to the viscous stress (Fig.4, b). The Marangoni stress profile can be divided into three parts, whose values are positive, nega-

tive and again positive, from the leading half-sphere to the trailing half-sphere. These three parts correspond respectively to a decrease, increase and decrease on the temperature profile. The variations between these parts (at angles θ equal to 70° and 145°) become sharper and sharper, implying a sudden directional change of the Marangoni force. Therefore, the liquid motion is consequently driven by the Marangoni effect, as shown by the comparison of the fields in Fig. 4a. Indeed without this effect, the motion driven by the viscous stress is similar to the Hill Vortex [9], whereas the two directional changes in the Marangoni stress profile yield three counter-rotating vortices. The resulting temperature field is strongly affected. The liquid motion remains stable even if the thermal gradient decreases during the evaporation. At angles θ equal to 70 and 180°, the colder liquid coming from the droplet surface is convected towards the droplet centre, whereas the hotter liquid coming from the droplet centre is convected towards the surface at the angle θ equal to 0 and 145°. Because of the absence of cooling inside the droplet, the local minima in the temperature profile remains at angles θ equal to 70 and 180°, whereas the local maxima occur at angles θ equal to 0 and 145°. The Marangoni stress profile and consequently the internal motion do not change. This internal motion effect on the surface temperature is consequently stronger than the effective heat flux which governs only the average droplet temperature. Consequently, the opposite influence of the temperature on the effective heat flux profile is significant, as soon as the surface temperature gradient increases.

Conclusion

The numerical simulation around acetone mondisperse droplet streams has yielded relevant results in agreement with the experimental data [16] and with the existing correlations of Virepinte [6] and Atthasit [7], concerning the vapor mole fraction field and the average transfer parameters. A refined analysis of the Marangoni effect on the internal motion and temperature field has been also proposed.

The results underline the relevance of the simulation regarding the physics and highlight the strong differences in the transfer parameters due to interaction effects. Corrections of the common correlations and improvement of the evaporation models are necessary to provide accurate results in combustions chambers, relying on parametric studies with this same numerical simulation in more severe environment. Otherwise, the study of the Marangoni effect in the cooling cases with the monodisperse droplets streams aims to predict precisely the temperature fields in the liquid phase: hence to improve the temperature measurements methods such as the rainbow refractometry, Laser Induced Fluorescence (LIF) and the infrared thermometry [6,7,10,11,16].

Acknowledgements

This work has been supported by the French environmental agency (ADEME) and the car manufacturer Renault for its contribution in improving the combustion in the engines and reducing the pollutants emissions. Further improvement have been carried out with support of the Deutsche Forschungsgemeinschaft (GRK 1114)

References

1. Renkzizbulut, M., and Haywood, R. J., Int. J. of Multiphase Flow, 14:189-202 (1988)
2. Ranz, W. E., and Marshall, W. R., Chem. Eng. Progr., 48:141-146, 48:173-180 (1952)
3. Mojtabi, M., Chadwick, N., Wigley, G., and Helie, J., ILASS, Como Lake, Italy, September 2008
4. Chiang, C. H., and Sirignano, W. A., Atomization and Sprays, 3:91-107 (1993)
5. Chiang, C. H., and Sirignano, W. A., Int. J. of Heat and Mass Transfer, 36:875-886 (1993)
6. Virepinte, J. F., Magre, P., Collin, G., Lavergne, G. and Biscos, Y., Comb. Science & Tech., 150:143-159 (2000)
7. Atthasit, A., Doue, N., Biscos, Y. and Lavergne, G., 1st Int. Symposium on Combustion and Atmospheric Pollution, St Petersburg, Russia, 2003
8. Leiroz, J. K., and Rangel, R. H., 8th International Symposium on Transport Phenomena in Combustion, San Francisco, USA, 1995
9. Abramzon, B., and Sirignano, W. A., Int. Journal of Heat and Mass Transfer, 32:1605-1618 (1989)
10. Castanet, G., and Lemoine, F., 31st Int. Symposium on Combustion, Heidelberg, Germany, 2006, pp. 2141-2148
11. Castanet, G., Maqua, C., Orain, M., Grisch, F., Lemoine, F., Int. Journal of Heat and Mass Transfer, 50:3670-3683 (2007)
12. Niazmand, H., Shaw, B. D., Dwyer, H. A. and Aharon, I., Comb. Science & Technology, 103:219-233 (1994)
13. Dwyer, H. A., Stapf, P., and Maly, R., Combustion and Flame, 121:181-194 (2000)
14. Fluent Inc. Copyright, http://www.fluent.com; OpenCFD Ltd., http://www.opencfd.co.uk/index.html
15. Guermond, J. L., Minev, P., and Shen J., Comput. Methods Appl. Mech. Eng., 195:6011-6045 (2006)
16. Frackowiak, B., Strzelecki, A. and Lavergne, G., Experiment in Fluids, in press (2008)

Table 1. Experimental parameters

	Cooling case 1	Cooling case 2
Injection temperature	22.4°C	45.6°C
Droplets diameter	173 µm	238 µm
Spacing parameter C	2.00	3.76
Ambient temperature	22.4°C	23.5°C
Droplet velocity	7.87 m/s	8.30 m/s
Distance L_{min}	30 mm	40 mm
Distance L_{max}	40 mm	50 mm

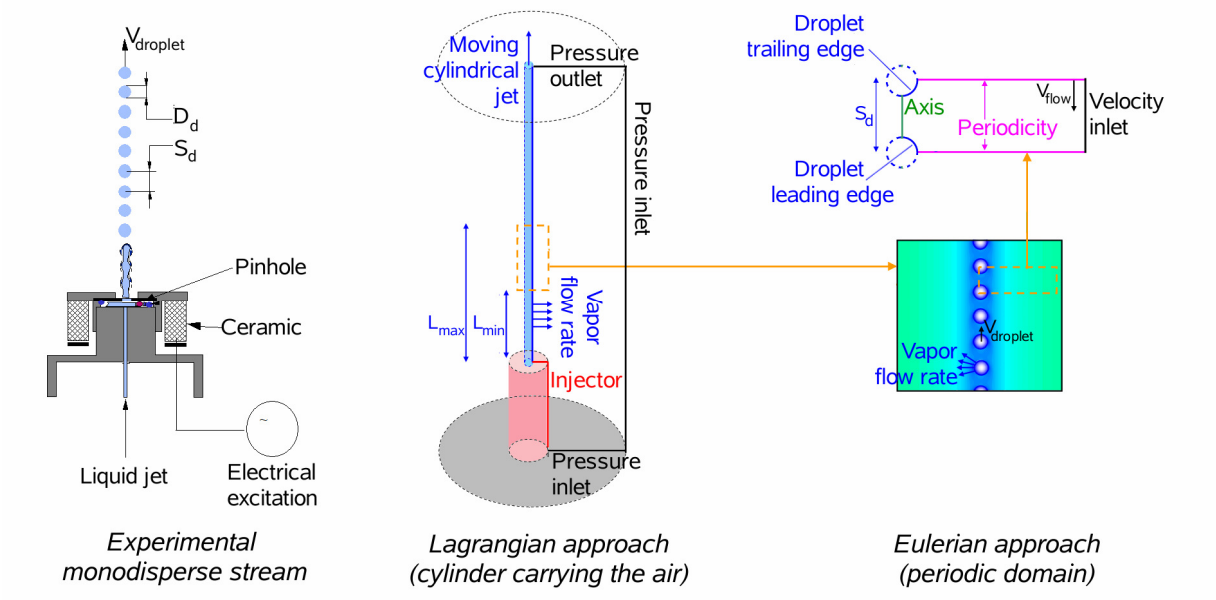

Figure 1. Monodisperse droplet stream: experimental device and proposed simulations

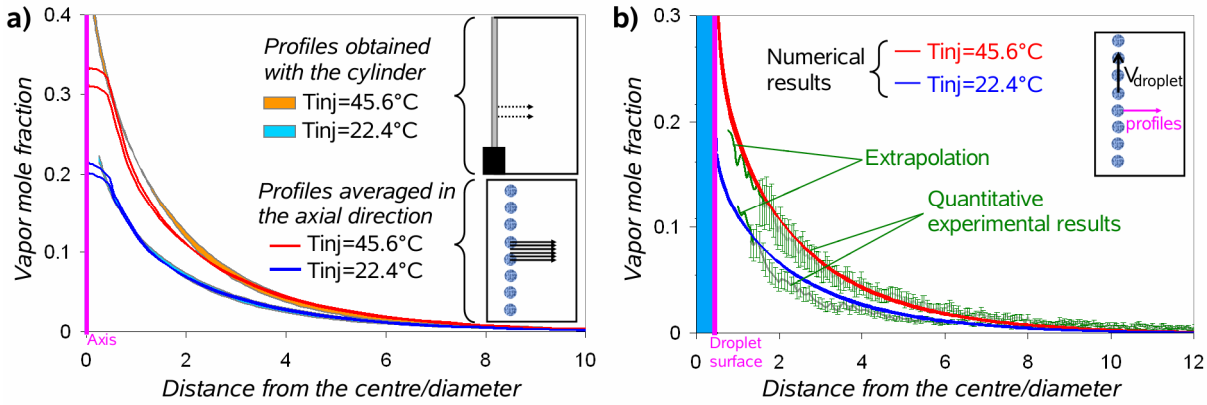

Figure 2. Acetone vapor mole fraction profiles. a) Comparison between the moving cylinder and the periodic domain. b) Comparison between the numerical and experimental results

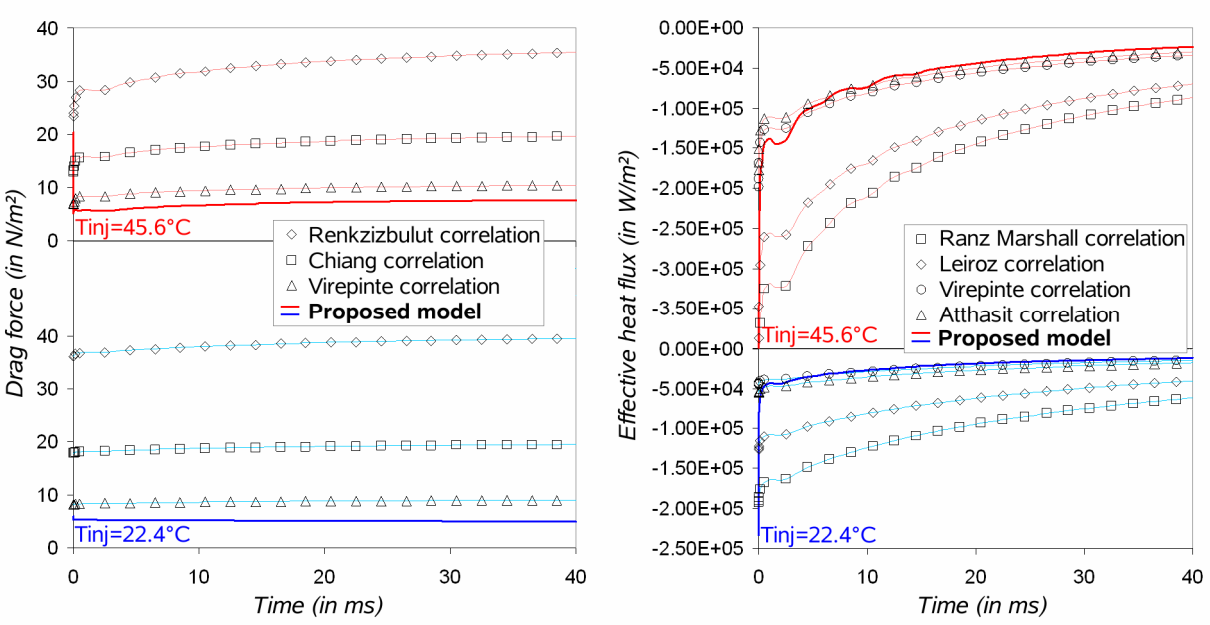

Figure 3. Non-dimensionnal drag force and effective heat flux evolution. Comparison with common correlations.

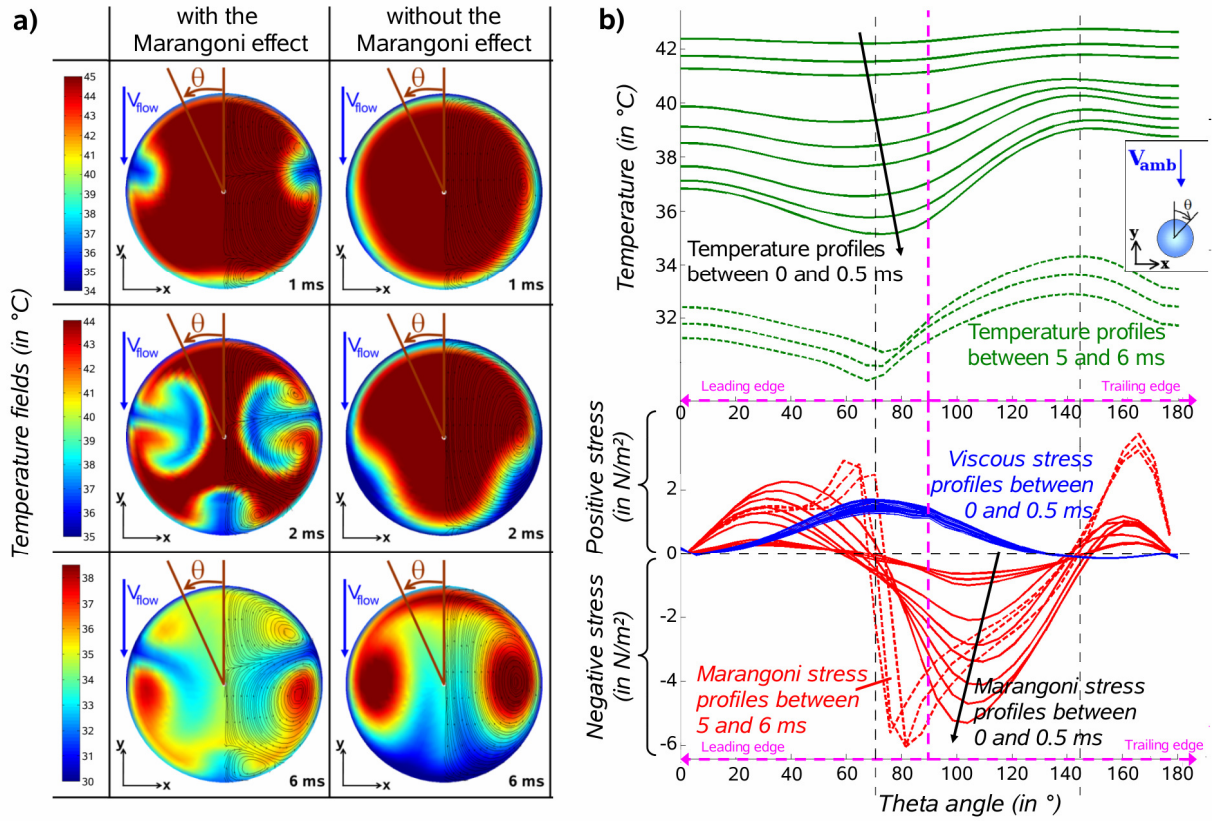

Figure 4. a) Temperature fields inside the droplet. b) Temperature and stress profiles on the droplet surface.